

Distribution Agreement

In presenting this thesis as a partial fulfillment of the requirements for a degree from Emory University, I hereby grant to Emory University and its agents the non-exclusive license to archive, make accessible, and display my thesis in whole or in part in all forms of media, now or hereafter now, including display on the World Wide Web. I understand that I may select some access restrictions as part of the online submission of this thesis. I retain all ownership rights to the copyright of the thesis. I also retain the right to use in future works (such as articles or books) all or part of this thesis.

Elena Mishkovsky

April 10, 2023

ELAVL3 Cryptic Exon Inclusion and Pathological TDP-43 in ALS/FTD

by

Elena Mishkovsky

Dr. Gary Bassell
Adviser

Neuroscience and Behavioral Biology

Dr. Gary Bassell
Adviser

Dr. Zachary McEachin
Committee Member

Dr. Anita Corbett
Committee Member

2023

ELAVL3 Cryptic Exon Inclusion and Pathological TDP-43 in ALS/FTD

By

Elena Mishkovsky

Dr. Gary Bassell

Adviser

An abstract of
a thesis submitted to the Faculty of Emory College of Arts and Sciences
of Emory University in partial fulfillment
of the requirements of the degree of
Bachelor of Science with Honors

Neuroscience and Behavioral Biology

2023

Abstract

ELAVL3 Cryptic Exon Inclusion and Pathological TDP-43 in ALS/FTD

By Elena Mishkovsky

Amyotrophic lateral sclerosis (ALS) is a fatal neurodegenerative disease which causes the degeneration of both upper and lower motor neurons and leads to progressive muscle weakness. Approximately 5-50% of patients with ALS are also diagnosed with frontotemporal dementia (FTD), a form of dementia which leads to poor decision-making and altered personality characteristics. The most common genetic form of this comorbidity, *C9orf72*-linked ALS/FTD, has been previously found to contain TDP-43 pathology in the majority of patient cases. TDP-43, an RNA-binding protein integral to RNA processing, was found to have a loss-of-function and a gain-of-toxicity due to its mislocalization, hyper-phosphorylation, and perinuclear aggregation. Previous data from the Bassell lab found that the loss of cellular TDP-43 leads to RNA misprocessing events and identified the presence of cryptic exons in the *ELAVL3* gene. Thus, this thesis aimed to examine the relationship between TDP-43 pathology and *ELAVL3* cryptic exons, with the hypothesis that a cytoplasmic aggregation of TDP-43 leads to the inclusion of cryptic exons in mRNA transcripts as a result of alternative splicing events. Among results, we found that the knockdown of TDP-43 in iPS-derived motor neurons leads to the inclusion of cryptic exons, TDP-43 pathology is present in hippocampal FTD patient tissue with *ELAVL3* cryptic exons present, and the expression of *ELAVL3* cryptic exons in patient tissue samples is correlated with high phosphorylated TDP-43 pathology. These results present novel evidence of the mechanisms behind *ELAVL3* cryptic exon presence in ALS/FTD, as well as insight into the relationship between TDP-43 pathology and *ELAVL3* cryptic exon occurrence in TDP-43 proteinopathies.

ELAVL3 Cryptic Exon Inclusion and Pathological TDP-43 in ALS/FTD

By

Elena Mishkovsky

Dr. Gary Bassell

Adviser

A thesis submitted to the Faculty of Emory College of Arts and Sciences
of Emory University in partial fulfillment
of the requirements of the degree of
Bachelor of Science with Honors

Neuroscience and Behavioral Biology

2023

Acknowledgements

My initial thanks goes to my adviser Dr. Gary Bassell for providing me with the mentorship and resources necessary to produce this thesis. I would also like to thank my research mentor Dr. Zachary McEachin for his guidance, encouragement, patience, and support during the research process. Additionally, I thank Dr. Nisha Raj for her advice during my research, as well as Mingee Chung for his collaboration on my work. Finally, I acknowledge Dr. Anita Corbett for providing assistance and feedback on my thesis, as well as the members of the Bassell Lab for their support in the laboratory.

Table of Contents

Introduction.....	1
Methods.....	7
Results.....	10
Discussion.....	13
Future Directions.....	18
Figures.....	20
Fig. 1.....	20
Fig. 2.....	21
Fig. 3.....	22
Fig. 4.....	23
Table 1.....	23
Fig. 5.....	24
References.....	25

Introduction

Amyotrophic Lateral Sclerosis (ALS)/ Frontotemporal Dementia (FTD): General Etiology

Amyotrophic Lateral Sclerosis (ALS), also known as Lou Gehrig's Disease, is a chronic fatal neurodegenerative disease characterized by the loss of both upper and lower motor neurons in the brain and spinal cord, with an average onset at about 50 years of age (Prasad et al., 2019). More specifically, neurodegeneration can occur in the motor cortex of the brain, as well as in the anterior horn of the spinal cord and brainstem nuclei (Masrori et al., 2020). Symptoms include decreased muscle mass and progressively weaker muscles, as well as issues with language and executive dysfunction in about 50% of ALS cases. The most important nature of the disease relates to the extremely short lifespan of patients with ALS as compared to patients with other neurodegenerative diseases: ALS patients are estimated to live between 1-5 years after the onset of the disease due to the degeneration of respiratory muscles and eventual respiratory failure. The majority of ALS cases are sporadic, or not genetically inherited, and about 10% of cases are found to be inherited from family members via an autosomal dominant pattern (Phukan et al., 2007). The lack of a cure or effective treatments for ALS, coupled with its extremely quick progression and severe symptoms, has caused the disease to remain a large focus of neurodegenerative disease research, as well as the main topic of this thesis.

Anywhere from 5 to 50% of patients with ALS are also diagnosed with frontotemporal dementia (FTD) (Lomen-Hoerth et al., 2003; Masrori et al., 2020; Phukan et al., 2007). When the two diseases are diagnosed together, this comorbidity is referred to clinically as ALS/FTD. The form of FTD most often diagnosed with ALS is bvFTD, or behavioral variant FTD; in this form, patients receive a clinical diagnosis based on personality changes and altered or poor decision-making (Mendez et al., 2013). After Alzheimer's Disease, FTD is the second most common form

of dementia (diagnosed in approximately 15-22 individuals per 100,000) (Onyike and Diehl-Schmid, 2014).

C9orf72-linked ALS/FTD

The onset of genetic ALS has been linked to mutations in several human genes, including *C9orf72*, *SOD1*, *TARDBP*, *NEK1*, and *UBQLN1* (Ghasemi and Brown, 2018). In 2011, however, it was discovered that the *C9orf72* mutation with a hexanucleotide repeat expansion (GGGGCC) in the chromosome 9 open reading frame 72 (*C9orf72*) gene is the most common cause of ALS and FTD; as such, this is often referred to as *c9ALS/FTD* (DeJesus-Hernandez et al., 2011). DeJesus-Hernandez et al. also found that this repeat expansion was present in the majority of families with TDP-43 pathology and a combined ALS/FTD phenotype, suggesting the importance of the *C9orf72* gene in causing ALS/FTD. Specifically, *c9ALS/FTD* is most often associated with sporadic behavioral variant FTD (bvFTD), where the patient may develop delusions or a deterioration of personality (Cooper-Knock et al., 2014). The wild-type *C9orf72* encoded protein regulates pre-mRNA splicing and transcription, as well as membrane traffic via the Rab GTPase protein family (Ghasemi and Brown, 2018). Therefore, mutations in the gene can cause impaired nucleocytoplasmic transport and/or the formation of aggregates due to stress granules (Ghasemi and Brown, 2018).

TDP-43 Pathology

In the 1990s, researchers discovered that ubiquitin inclusions were present in patients with both ALS and FTD. Specifically, these inclusions consist of the TAR DNA binding protein 43, or the TDP-43 protein encoded by the *TARDBP* gene (Arai et al., 2006; Neumann et al.,

2006). Neumann et al. demonstrated that TDP-43 is a major pathological protein in both ALS and FTLD; in particular, the pathological form of the TDP-43 protein is ubiquitinated and hyperphosphorylated. This represented a major breakthrough in understanding the molecular relationship between ALS and FTD, as well as a way of identifying a shared pathology between these diseases. Neurodegenerative diseases (such as ALS/FTD) with TDP-43 pathology are often referred to as TDP-43 proteinopathies (Dugger and Dickson, 2017).

TDP-43 is an RNA-binding protein integral to RNA processing, which binds to members of the heterogeneous nuclear riboprotein (hnRNP) family during processing (eg. for splicing inhibitory activity) (Buratti et al., 2005; Mackenzie and Rademakers, 2008; Wang et al., 2004). Wild-type TDP-43 is localized in the nucleus in cells including neurons (i.e. in people not diagnosed with ALS or other neurodegenerative diseases). However, in disease cases, TDP-43 may be mislocalized to the cytoplasm of a neuron where it can become aggregated and hyperphosphorylated. Previously, it was thought that this perinuclear aggregation of pathological TDP-43 was the basis for its toxicity through a toxic gain-of-function mechanism (Kabashi et al., 2010; Shodai et al., 2013). It has also been posited that the ubiquitinated and hyperphosphorylated nature of TDP-43 deposits in the brain and spinal cord of patients with ALS/FTD causes the deposits to act as inclusion bodies, giving them an almost prion-like nature (Hasegawa et al., 2008; Prasad et al., 2019). However, recent studies have suggested that due to the role of TDP-43 in RNA processing, the mislocalization of TDP-43 may instead result in a loss of nuclear function (Kabashi et al., 2010; Schwenk et al., 2016).

Preliminary data from the Bassell lab demonstrated that the mislocalization of TDP-43 from the nucleus causes the protein to lose its RNA processing function, resulting in splicing errors or altered mRNA processing events (McEachin, Z., unpublished). Thus, the three essential

pathological hallmarks of ALS/FTD include the mislocalization, phosphorylation, and perinuclear aggregation of the TDP-43 protein (Prasad et al., 2019). The aggregation of TDP-43 alone is estimated to be present in approximately 45% of FTLD cases and 97% of ALS cases (Ling et al., 2013). Overall, it is held that the “toxic” form of TDP-43 (which in this thesis will signify its mislocalization, phosphorylation, and perinuclear aggregation) is a result of a toxic gain-of-function and a loss of correct RNA splicing function (Kabashi et al., 2010; Shodai et al., 2013). As ALS and FTD are commonly diagnosed together and both contain these pathological hallmarks, this research has focused on examining the mechanisms by which TDP-43 is mislocalized in *C9orf72*-linked ALS/FTD.

Role of Cryptic Exons in Neurodegeneration

While cassette exons are a result of alternative splicing (about 50-60% of all splicing events), cryptic exons are a product of incorrectly-spliced mRNA due to alternative splicing events (Dvinge and Bradley, 2015). Cassette exons may be either included in or spliced out of an mRNA transcript, resulting in multiple possible protein isoforms. Cryptic exons, however, may be included in transcripts during splicing events that are improperly regulated by RNA-binding proteins, resulting in novel transcript variants that may be either degraded or translated to produce truncated or non-functional proteins. Truncated proteins may be the result of the addition of premature stop codons in transcripts containing a cryptic exon. This phenomenon is due to the nature of these exons as “cryptic”: these exon sequences are omnipresent in the RNA, however they are usually repressed with the presence of an RNA-binding protein, such as wild-type TDP-43.

Previous studies have also demonstrated that pathological TDP-43 does not repress the inclusion of cryptic exons in ALS/FTD as its wild-type form does, due to cytoplasmic aggregation and mislocalization from the nucleus of a neuron (i.e. loss of RNA-binding protein function) (Ling et al., 2015; Klim et al., 2019). In 2015, Ling et al. found that the depletion of TDP-43 from embryonic mouse stem cells led to disrupted mRNA translation and nonsense-mediated decay as a result of cryptic exon inclusion (Ling et al., 2015). Notably, another recent study found that TDP-43 represses the inclusion of cryptic exons in the *UNC13A* gene for ALS/FTD (Ma et al., 2022). Thus, wild-type TDP-43 is a necessary repressor of cryptic exon inclusion during alternative splicing events and the pathological version plays an important role in the pathogenesis of ALS/FTD. Preliminary data from the Bassell lab has led to our interest in cryptic exons, as it was determined previously by Dr. Zachary McEachin that knockdown of TDP-43 in iPS-derived motor neurons (iPS-MNs) leads to the inclusion of cryptic exons in mRNA transcripts during splicing (McEachin, Z., unpublished).

ELAVL3 Cryptic Exons in ALS/FTD

The ELAVL family comprises a group of similar RNA-binding proteins that regulate post-transcriptional gene expression (Soller and White, 2004). The ELAVL family (embryonic lethality and abnormal visual system) was discovered in *Drosophila melanogaster*, yet it is also present in humans (eg. the Hu gene family) (Cai et al., 2022; Lee et al., 2021). Of the *ELAVL* group, there are four subtypes: *ELAVL1* is expressed in many cell types while *ELAVL2*, *ELAVL3*, and *ELAVL4* are expressed only in neurons (Cai et al., 2022). ELAVL3, specifically, is an RNA-binding protein associated with synaptic and axonal structures which regulates splicing and polyadenylation (changes to 3' UTR lengths) (Ogawa et al., 2018). Importantly, *ELAVL3* is also

implicated in various neurological disorders and it has eluded the focus of many cryptic exon studies. Loss of the ELAVL3 protein in a neuron can lead to cellular dysfunction or degeneration by resulting in downstream alternatively-spliced genes which can create a harmful, dysfunctional, or truncated protein (Diaz-Garcia et al., 2021). Diaz-Garcia et al. recently found that ELAVL3 is downregulated (depleted from the nucleus) in sporadic ALS spinal cord patient tissue, and results in a shorter protein isoform (Diaz-Garcia et al., 2021).

Changes in 3' UTR lengths may also occur, as well as alternative polyadenylation (APA), via disruption of the polyadenylation signal (Grassi et al., 2019; Lee et al., 2021). As both 3' UTRs and alternative polyadenylation are imperative to RNA localization and stability, ELAVL3 loss may lead to RNA misprocessing events where a neuron may become more stable, unstable, mislocalized, or degraded. Preliminary research from this lab identified the presence of cryptic exons in the *ELAVL3* gene between exons 3 and 4, with *STMN2* as a control (a gene already known to contain cryptic exons) (McEachin, Z., unpublished). This contrasts with a previous study which found no evidence of cryptic exons in an RNA sequencing read between exons 3 and 4 of the *ELAVL3* gene (Diaz-Garcia et al., 2021). Additional analyses of the sequencing flanking the cryptic exon in *ELAVL3* revealed UG repeat motifs, a known binding motif of TDP-43 (Polymenidou et al., 2011; Tollervey et al., 2011). From this information, we gained interest in examining the role of *ELAVL3* cryptic exons in ALS/FTD pathogenesis.

Research Aims

In this research, we aimed to examine how the inclusion of cryptic exons in *ELAVL3* contributes to disease pathogenesis in TDP-43 proteinopathies (specifically in ALS/FTD). We hypothesized overall that the loss of TDP-43 in human brain tissue and iPS-MNs leads to a

reduction in ELAVL3 expression due to the inclusion of cryptic exons. Because of the nature of wild-type TDP-43 as a repressor of cryptic exons, we hypothesized that a cytoplasmic aggregation of TDP-43 (and thus a loss of its nuclear RNA-binding protein function due to its nuclear depletion) would lead to alternative splicing events where *ELAVL3* cryptic exons are included in the mRNA transcript in ALS/FTD cases (see Fig. 5). As a result, the overall expression of wild-type ELAVL3 should be reduced due to the production of truncated or degraded proteins. This would also likely lead to genome-wide changes in polyadenylation (i.e. changes at the 3' UTR) due to the nature of the *ELAVL3* binding motif and based on previous work on the function of ELAVL3. Our goals included confirming the presence of *ELAVL3* cryptic exons in human ALS/FTD disease cases (and its presence in neurons with TDP pathology), as well as determining whether there is a correlation between *ELAVL3* cryptic exon expression and pTDP-43 abundance in human disease case tissues.

First, we aimed to validate the presence of *ELAVL3* cryptic exons in human tissue samples and iPS-derived motor neurons via qPCR and RT-PCR, respectively. Second, we aimed to detect the presence of *ELAVL3* cryptic exons in patient brain tissue with phosphorylated TDP-43 (pTDP-43) pathology via *in situ* hybridization (BaseScope). Third, we aimed to measure pTDP-43 abundance in human frontal cortex samples to determine if *ELAVL3* cryptic exon expression correlates with pTDP-43 abundance in the frontal cortex of FTLD-TDP cases (via insoluble fraction and ELISA immunoassay). A future goal is to define transcriptomic changes associated with *ELAVL3* loss via RNA sequencing following mediated depletion of TDP-43.

Methods

Cell Culture

SH-SY5Y neuroblastoma cells were cultured in Gibco Dulbecco's Modified Eagle Medium/Nutrient Mixture F-12 (DMEM/F-12) with 1% PenStrep and 10% fetal bovine serum (FBS) as nutritional supplements. Induced pluripotent stem cell lines (iPSCs) were cultured in mTeSR (Stem Cell Technologies) and maintained on matrigel-coated plates. iPSCs were passed every 4-5 days with ReLeSR (Stem Cell Technologies).

siRNA Transfection

SMARTpool siRNAs (Dharmacon) were transfected targeting *TARDBP* or *ELAVL3* genes at 40nM with lipofectamine RNAiMax in SH-SY5Y cells. These were plated at 450K cells per well in a 12-well plate. Media was changed 24 hours after transfection and cells were harvested 48 hours after transfection. For siRNA-mediated reduction of *TARDBP* or *ELAVL3* in iPS-MNs, we performed gymnotic delivery of Accell siRNAs (Dharmacon) at 1 μ M. Media was changed 72 hours after the reduction and cells were harvested 96 hours after reduction.

Lysate Preparation and Western Blots

Cells were lysed in a 2% SDS buffer with HALT protease and phosphatase inhibitors (Thermo Fisher). Lysates were sonicated for 3 cycles of 4 sec on/3 sec off at 30% amplitude. Protein lysate quantification was done using a BCA assay. Proteins for Western blots were prepared in a 4x loading buffer and heat-denatured at 70°C for 15 minutes. On 10% Bis-Tris gels (Thermo Fisher), lysates were normalized to equal amounts. They were then resolved on 10% Bis-Tris gels (Thermo Fisher), transferred to 0.44 mm PVDF membranes, and blocked in Li-Cor Odyssey blocking buffer (Li-Cor) for 1 hour. Membranes were incubated overnight at 4°C with primary antibodies diluted in blocking buffer. Secondary antibodies were then diluted in more

blocking buffer and applied to the membrane for 1 hour at room temperature. Primary antibodies used in immunoblotting experiments included anti-TDP (1:1000, Proteintech), anti-ELAVL3 (1:1000, Abnova), and anti-GAPDH (1:5000, Cell Signaling).

RNA extraction

RNA was extracted from cells and human postmortem tissues using 1mL Trizol, which was followed by column cleanup using Zymo Miniprep RNA kit (Zymo). For cell culture, cells were rinsed once in ice cold PBS and 1mL Trizol was then added. Approximately 30mg of human postmortem tissue was homogenized in 1mL Trizol using the Bullet Blender (NextAdvanced).

cDNA Reverse Transcription and Quantitative Polymerase Chain Reaction (qPCR)

500 ng samples of RNA were converted to cDNA using a High Capacity cDNA Reverse Transcription Kit (Thermo Fisher). cDNA was diluted with 20uL of RNase-free water. qPCR was performed for each sample using TaqMan probe chemistry. We assessed the expression of these genes using premade TaqMan probes for both *TARDBP* and *ELAVL3*. To assess *ELAVL3* cryptic exon inclusion, a custom TaqMan probe targeting the *ELAVL3* cryptic exon was used. Relative tissue RNA was normalized to *GAPDH*.

In situ Hybridization (ISH)

Using BaseScope, *in situ* hybridization was performed. We used custom BaseScope probes targeting the *ELAVL3* exon 3-cryptic exon junction as well as exon 3-exon 4 junction.

These probes were designed by and purchased from ACDBio. *In situ* hybridizations were performed as per the manufacturer's protocol.

Immunohistochemistry

Immunohistochemistry (IHC) was performed using paraffin-embedded FTLD-TDP and control hippocampal tissue slices. Samples were deparaffinized for 18 min and antigen retrieval was done for 30 min. All reagents used were Dako IHC blocking reagents. Samples were blocked for 30 min and then primary and secondary antibodies (Cosmo Bio S409/410 targeting pTDP-43) were applied for 45 min and 30 min, respectively. DAB chromogen was used as an assay (5 min).

Insoluble Fraction

pTDP-43 protein abundance was measured in human postmortem FTLD-TDP frontal cortex tissue. Frozen tissue samples were cut to approximately 50-60 mg and stabilized in approximately 250 μ L (1:5 w/v) RIPA buffer. Samples were sonicated at 3 cycles of 3 sec on/3 sec off at 30% amplitude for a total of 9 sec on. The protein concentration of C9ALS/FTD cases was then measured by BCA assay. Approximately 220 samples were prepared and a pilot study of C9ALS/FTD cases was completed, while the rest of the samples are in progress.

Results

A preliminary analysis from the Bassell Lab of several differentially expressed genes known to contain cryptic exons identified *ELAVL3* among them (Fig. 1B) after a depletion of

TDP-43 in iPS-MNs (Fig. 1A) (McEachin, Z. et al., unpublished). *ELAVL3* was among the most decreased transcripts, along with *TARDBP* and *STMN2* (already known to contain cryptic exons) (Fig. 1B). A subsequent RNA sequencing read confirmed the presence of cryptic exons with TDP siRNA (si*TARDBP*) (Fig. 1C).

Knockdown of TDP-43 Leads to the Inclusion of Cryptic Exons

In order to identify RNA misprocessing events associated with TDP-43 loss, preliminary data was generated by knocking down TDP-43 in iPS-derived motor neurons. Six days after cell plating, TDP-43 was knocked down in three different iPS-MN lines. These knockdowns were performed with either control/scrambled siRNA or TDP siRNA. RNA was extracted, and 500 ng samples were converted to cDNA. Polymerase chain reaction (PCR) was performed to amplify and detect (by DNA electrophoresis) the presence of a cryptic exon within the cDNA. For this, we used primers that hybridized specifically to the *ELAVL3* cryptic exon sequence. RNA sequencing and alternative splicing analysis were then performed.

Reverse transcription polymerase chain reaction (RT-PCR) data reveals the presence of cryptic exons in genes with TDP-43 depleted from iPS-MNS; *CAMK2B*, *STMN2*, and *GRAMD1A* are used as controls, as they were previously known to contain cryptic exons in their pathological forms (Fig. 2A). Bands indicative of cryptic exons are detectable for all three lines of iPS-MNs with siRNAs targeting *TARDBP*, demonstrating the clear presence of cryptic exons in all four genes, including *ELAVL3*. The isolation of an *ELAVL3* band and subsequent Sanger sequencing also reveal the presence of a probable premature stop codon in the RNA sequence, indicating the presence of a cryptic exon between exon 3 and exon 4 (Fig. 2B).

TDP-43 Pathology: in situ Hybridization and Immunolabeling of Cryptic Exon Patient Tissue

For *in situ* hybridization and immunohistochemistry, we used paraffin-embedded slides containing hippocampal slices of either control or FTLD-TDP tissue. Hippocampal tissue was used due to the fact that the hippocampus has robust pathological TDP-43 burden; it also has a clear architecture, making it easy to identify tissues with cells containing TDP-43 pathology. It is important to note that FTLD, and not ALS, results in hippocampal TDP-43 pathology. *In situ* hybridization was performed with custom probes targeting both the *ELAVL3* exon 3-exon 4 junction and the exon 3-cryptic exon junction. An antibody targeting phosphorylated TDP-43 (S409/410) was used to assess pTDP-43 aggregates via immunohistochemistry. The tissue was counterstained with hematoxylin to identify neuronal nuclei.

Images of the *in situ* hybridizations show clear TDP-43 pathology in disease cases versus control cases. The FTLD-TDP case exhibits staining for pTDP-43, *ELAVL3*, and *ELAVL3* cryptic exons, as expected for a disease case (see Fig. 3). *ELAVL3* is stained in both control and FTLD-TDP cases, confirming the presence of wild-type *ELAVL3* in a non-disease human case. pTDP-43 and *ELAVL3* cryptic exon transcripts are detected only in the FTLD-TDP case and not in the control case. It is also interesting to note from these images that 1) many FTLD-TDP neurons seem to contain a single cryptic exon-containing RNA transcript while others appear to have 2 or 3, 2) pTDP-43 pathology and *ELAVL3* cryptic exon inclusions may not occur in the same cell, and 3) these RNA cryptic exon-containing transcripts appear to be retained in the nucleus. This last observation is notable due to the nature of pathological TDP-43, which is to be mislocalized to the cytoplasm.

Correlation Between pTDP-43 Pathology and ELAVL3 Cryptic Exon Presence

Using a similar protocol as we did for the RT-PCRs, we converted 500 ng samples of RNA to cDNA (reverse transcription) and performed quantitative polymerase chain reactions (qPCRs) on 129 samples of cDNA using premade TaqMan probes to detect *ELAVL3* and *TARDBP* transcripts. A custom TaqMan probe targeting the *ELAVL3* cryptic exon was also used to examine the inclusion of *ELAVL3* cryptic exons; these probes were used to quantify the relative cryptic exon expression in each case. *GAPDH* served to normalize relative tissue RNA. For this analysis, 129 patient tissue samples of the frontal cortex BA9 region were used.

We found that the expression of *ELAVL3* cryptic exons in genes correlates with higher pTDP-43 pathology (one-way ANOVA, * $p < 0.05$, $n = 129$) (Fig. 4). More specifically, this correlation was detected in patient disease cases (Table 1), including those with C9ALS/FTD, C9FTD, granulin (GRN-related FTLD), and sporadic FTLD (sFTLD); all of these cases contain higher relative *ELAVL3* cryptic exon expression. There is a clear and marked difference presented between patient cases with pTDP-43 pathology and those without pTDP-43 pathology (control, C9ALS, FUS) (see Fig. 4B). Disease cases with known pTDP-43 pathology contain much higher levels of relative *ELAVL3* cryptic exon expression, while cases without pTDP-43 pathology contain little to no *ELAVL3* cryptic exon expression.

Discussion

In 2006, studies revealed that pathological TDP-43 occurs in both ALS and FTLD, and that TDP-43 can be both hyper-phosphorylated and ubiquitinated (Neumann et al., 2006); this motivates our research. Recent work from the Bassell lab has also demonstrated several other breakthroughs in this research (McEachin, Z. et al., unpublished). First, it was found that the

mislocalization of TDP-43 causes it to have a loss-of-function and result in splicing errors, a phenomenon that has been described by others as well (Klim et al., 2019; Ling et al., 2015). Second, the loss of TDP-43 in iPS-MNs leads to the inclusion of cryptic exons in mRNA transcripts as a result of alternative splicing events. Third, the presence of cryptic exons in the *ELAVL3* gene was identified (see Fig. 1). These three findings have led to the premise of this thesis, which aims to understand how the inclusion of *ELAVL3* cryptic exons contributes to disease pathogenesis in ALS/FTD. These findings are also significant because there are limited published studies investigating the relationship between *ELAVL3* cryptic exon inclusion and TDP-43 pathology in ALS/FTD pathogenesis. The hypothesis that the loss of TDP-43 in iPS-MNs and human brain tissue leads to the inclusion of *ELAVL3* cryptic exons and a subsequent reduction in *ELAVL3* expression was ultimately supported by the data found during this thesis work. The findings in this research also provide some of the first visual evidence of cryptic exon inclusion in the *ELAVL3* gene, as well as important insight into the relationship between TDP-43 proteinopathies and *ELAVL3* cryptic exons.

First, we found that a knockdown of the TDP-43 protein in iPS-derived motor neurons leads to the inclusion of cryptic exons in mRNA transcripts. Reverse transcription polymerase chain reaction data in three different lines of iPS-MNs demonstrated the presence of cryptic exons in the *ELAVL3* gene for all three cell lines (Fig. 2A). The presence of a cryptic exon was specifically denoted between exon 3 and exon 4 in the *ELAVL3* Sanger sequencing reading (see Fig. 2B). These data support our hypothesis and can be explained by the RNA-binding protein function of TDP-43. Wild-type TDP-43 binds to the UG repeat motifs RNA sequence on the *ELAVL3* gene directly before exon 3 and represses the splicing of the cryptic exon in *ELAVL3* (Fig. 5A) (Ma et al., 2022; Polymenidou et al., 2011; Tollervey et al., 2011).

Loss of TDP-43 via mislocalization from the nucleus of the neuron to the cytoplasm, and therefore the loss of its function, constitutes an additional gain-of-toxicity function whereby the inclusion of cryptic exons in the *ELAVL3* gene is no longer repressed due to alternative splicing events (Fig. 5B). Thus, an additional consequence is the reduced expression of *ELAVL3* as well. This first experiment yielded similar results to those of two prior studies. Ling et al. found that the depletion of TDP-43 from mouse embryonic cells impaired the repression of cryptic exons by promoting nonsense-mediated decay, however this experiment was not attempted in the *ELAVL3* gene nor in iPS-MNs (Ling et al., 2015). Ma et al. discovered a similar result in TDP-43 knocked down in the *UNC13A* gene in neuronal nuclei isolated from frontal cortices (Ma et al., 2022). However, this was again not explored in iPS-MNs or in *ELAVL3*, demonstrating the novelty of our research.

We next used *in situ* hybridization (BaseScope) and immunohistochemistry techniques to identify cryptic exons and TDP-43 pathology in patient brain tissue. Hippocampal tissue samples of control and FTLD-TDP tissue were used with three probes targeting pTDP-43, wild-type *ELAVL3*, and *ELAVL3* cryptic exons (Fig. 3). Control cases revealed the presence of only wild-type *ELAVL3* as expected, while disease cases contained wild-type *ELAVL3*, *ELAVL3* cryptic exons, and pTDP-43. pTDP-43 was also mislocalized from the nucleus, as is expected in neurons with pathological TDP-43. These results visually confirmed the presence of TDP-43 pathology in FTLD-TDP cases, as well as the inclusion of *ELAVL3* cryptic exons in a disease case with known TDP-43 pathology. As no other research study has examined the effects of TDP-43 knockdown on *ELAVL3* cryptic exons via *in situ* hybridization, these images provide some of the first visual evidence of *ELAVL3* cryptic exon inclusion in patient tissue with TDP-43 pathology.

Interestingly, the *in situ* hybridization images also revealed the presence of 2-3 cryptic exon transcripts in some nuclei, as opposed to only one in other nuclei. These RNA cryptic exon-containing transcripts also appear to be retained in the nucleus. This latter result may be explained in relation to nonsense-mediated decay, as some studies have posited that nonsense-mediated decay occurs in the nucleus of a cell (Apcher et al., 2013; Iborra et al., 2001). The fact that these cryptic exon-containing transcripts may be retained in the nucleus could mean that the inclusion of premature stop codons leads to nonsense-mediated decay in the nucleus instead of translation into a nonfunctional or harmful protein.

Finally, we found an important correlation between the presence of cryptic exons in the *ELAVL3* gene and pTDP-43 pathology. qPCR data from frontal cortex (BA9 region) patient samples revealed that the expression of *ELAVL3* cryptic exons is specifically found in cases with pTDP-43 pathology (one-way ANOVA, * $p < 0.05$, $n = 129$) (see Fig. 4). Patient disease cases (all with pTDP-43 pathology) showed high relative *ELAVL3* cryptic exon levels of accumulation (see Table 1), while cases without TDP-43 pathology contained little to no detectable *ELAVL3* cryptic exons. As phosphorylated TDP-43 is the pathological form of TDP-43 (whereby it is hyper-phosphorylated and considered “toxic”), a higher pTDP-43 pathology in cells would mean a loss-of-function of the protein and the inability to perform its RNA-binding function. Thus, a higher likelihood of *ELAVL3* cryptic exon inclusion can be expected. This result is significant due to the necessity of the correct functioning of the ELAVL3 protein; a reduction in *ELAVL3* gene expression may lead to further downstream changes in global splicing and polyadenylation and the progression of TDP-43 proteinopathy pathogenesis.

Diaz-Garcia et al. have recently examined the relationship between TDP-43 abnormalities in co-occurrence with ELAVL3 abnormalities and have determined that ELAVL3

is an important upstream RNA-binding protein in ALS pathogenesis (Diaz-Garcia et al., 2021). However, they presented different methodology, tissue samples, and results from those in this thesis. They primarily used human spinal cord tissue and mice, in addition to previously published data on laser-captured spinal motor neurons, to identify (via IHC and *ELAVL3* knockdown) the *ELAVL3* abnormalities in sporadic ALS, including the nuclear depletion of *ELAVL3* as a pathological hallmark. In contrast to our work, Diaz-Garcia et al. did not observe TDP-43 pathology in co-occurrence with *ELAVL3* abnormalities (although they mainly examined *SOD1* mutations). They also concluded that *ELAVL3* abnormalities were unrelated to TDP-43-dependent cryptic exons. Differences between this research and that in this research could possibly be due to the fact that Diaz-Garcia et al. focused on sporadic (and not genetic) ALS. Furthermore, our work was based on preliminary novel evidence of cryptic exon inclusion in the *ELAVL3* gene following TDP-43 knockdown, which contrasts with the evidence from Diaz-Garcia et al. (McEachin, Z. et al., unpublished).

Overall, the results from this thesis support our hypothesis that a cytoplasmic aggregation and nuclear depletion of TDP-43 leads to the inclusion of *ELAVL3* cryptic exons in mRNA transcripts in ALS/FTD cases. The presence of *ELAVL3* cryptic exons was found in iPS-MNs with TDP-43 knocked down, *ELAVL3* cryptic exons and TDP-43 pathology were found in hippocampal disease tissue, and a correlation between higher TDP-43 pathology and *ELAVL3* cryptic exon relative expression was found in disease cases. These results confirm the crucial nature of wild-type TDP-43 in regulating alternative splicing in neurons, as well as its newly-discovered role in regulating the expression of *ELAVL3*. The correct function of TDP-43 and *ELAVL3* are imperative to maintain healthy neuronal structure, and a loss of either of their functions may contribute to the pathogenesis in ALS/FTD.

Future Directions

Considering the nature of the results from this thesis work, several additional experiments may aid in the understanding of the mechanisms surrounding TDP-43 and ELAVL3 in the future. First, completing a full analysis of the relative abundances of phosphorylated TDP-43 in postmortem human brain tissue from *C9orf72* donors may be valuable. Quantifying pTDP-43 measurements may illuminate molecular cascade mechanisms that result from the dysfunction of pathological TDP-43. This experiment could provide particularly significant evidence, as no previous studies have correlated pTDP-43 protein abundance with various cryptic exons in disease-relevant brain regions. Although sequential biochemical fractionation (insoluble fraction) was begun during this thesis work (approximately 220 samples were collected), this work was not completed due to time and labor constraints with the exception of a smaller pilot study of C9ALS/FTD samples. A complete insoluble fraction analysis according to the methods outlined in this thesis would thus be beneficial in meeting the above goal.

In addition, performing a co-localization of TDP-43 and *ELAVL3* cryptic exons using *in situ* hybridization would be beneficial to understand the localization patterns shared by both pTDP-43 and *ELAVL3* cryptic exons. This analysis would also allow us to visualize patterns of co-occurrence between the two, and to perhaps quantify the percentage of cells in a given region with co-occurrence versus those without. This study could provide greater insight into the mechanisms behind how pTDP-43 pathology could lead to cryptic exon inclusion and the rates at which they co-occur, as the determining factors behind these mechanisms are currently unknown. From observation during this research and previous research by Dr. Zachary McEachin, it became apparent that there is variability in the expression of pTDP-43 pathology and *ELAVL3* cryptic exons from *in situ* hybridization staining. Utilizing probes that both detect

pTDP-43, as well as the *ELAVL3* exon 3-cryptic exon/cryptic exon-exon 4 junctions, on the same postmortem human hippocampal tissue would allow us to further examine the rates of co-localization of pTDP-43 and *ELAVL3* cryptic exons in FTD patient donor tissue.

Finally, performing a knockdown of wild-type *ELAVL3* in iPS-derived motor neurons in addition to paired RNA sequencing may allow us to identify changes in polyadenylation in the *ELAVL3* gene as a result of a reduction in expression. As the loss of wild-type *ELAVL3* can lead to cellular dysfunction or degeneration by changing the 3'UTR length (alternative polyadenylation), a knockdown of *ELAVL3* in iPS-MNs should presumably lead to this same result. Paired RNA sequencing would then allow us to confirm the function of wild-type *ELAVL3*, as well as to validate the change in 3'UTR length by comparing the wild-type *ELAVL3* 3'UTR to that of the cell with *ELAVL3* knocked down. No current published research has examined the knockdown of *ELAVL3* in iPS-derived motor neurons, nor the subsequent RNA sequencing; thus, these experiments would aid in providing a more complete understanding of the mechanisms behind alternative polyadenylation in the *ELAVL3* gene in TDP-43 proteinopathies.

Figures

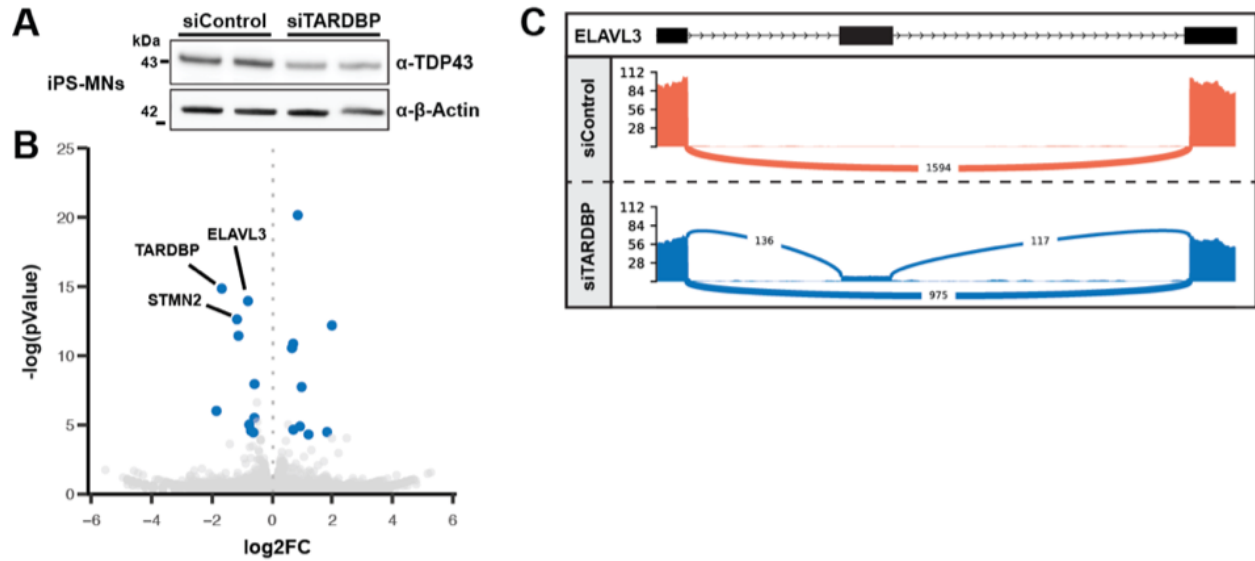


Fig. 1. Knockdown of TDP-43 in iPS-MNs identifies and confirms the presence of *ELAVL3* cryptic exons.

A) siTARDBP targeting TDP-43 demonstrates a lower abundance of TDP-43 than that of the housekeeping gene beta-actin, confirming the knockdown of TDP-43.

B) Most downregulated genes identified include *STMN2*, *TARDBP*, and *ELAVL3*, with *TARDBP* and *ELAVL3* being the most significant.

C) RNA sequencing reads demonstrate the presence of a cryptic exon in *ELAVL3* between exons 3 and 4.

(Figure provided by Dr. Zachary McEachin).

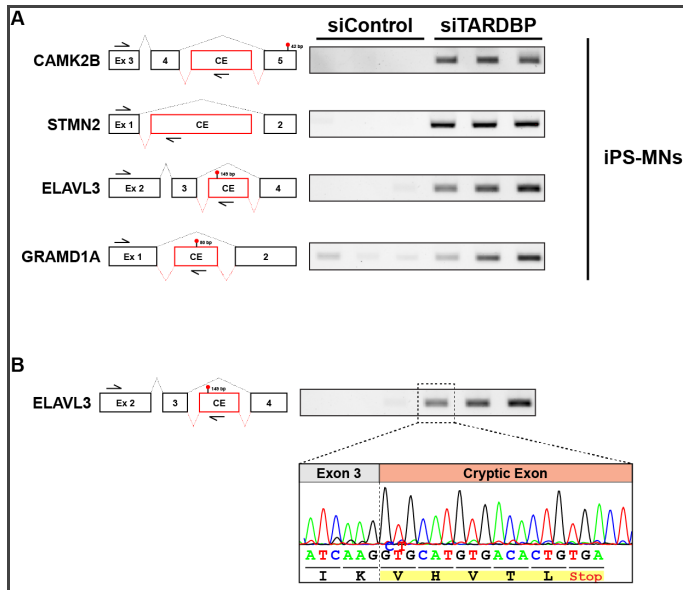


Fig. 2.

(A) Validation of *ELAVL3* cryptic exon presence in TDP-43 iPS-MNs. Controls include *CAMK2B*, *STMN2*, and *GRAMD1A* (previously known to have cryptic exons). N=3 for all siControl groups; n=3 for all siTARDBP groups.

(B) One *ELAVL3* band was excised and Sanger sequenced. A premature stop codon can be seen in the sequencing. N=1.

(Figure provided by Dr. Zachary McEachin).

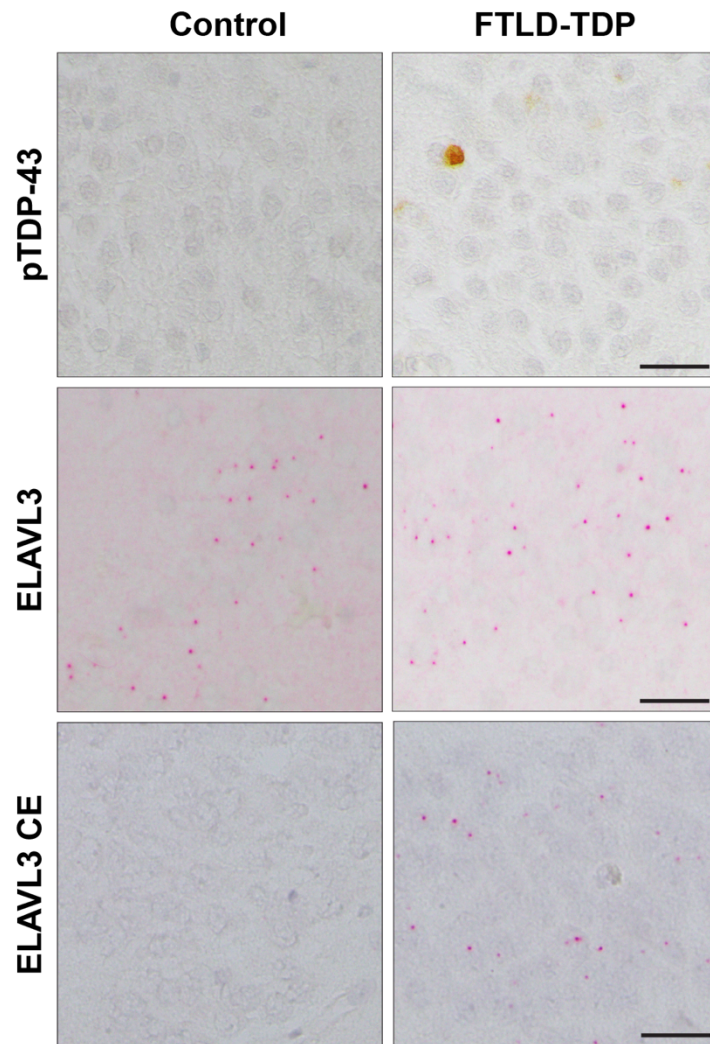


Fig. 3. *In situ* hybridization/IHC image staining for TDP-43 pathology in control versus FTLD-TDP disease cases. pTDP-43 (IHC, stained in orange) is present in FTLD-TDP cases but not in control cases. Wild-type *ELAVL3* (stained in red) is present in both control and FTLD-TDP cases. *ELAVL3* cryptic exons (stained in red) are detected in FTLD-TDP cases but not control cases. pTDP-43 is mislocalized from the nucleus and *ELAVL3* transcripts are retained in the nucleus. Scale bars: 25 μ m; n=6. (Data collected in collaboration with Mingee Chung).

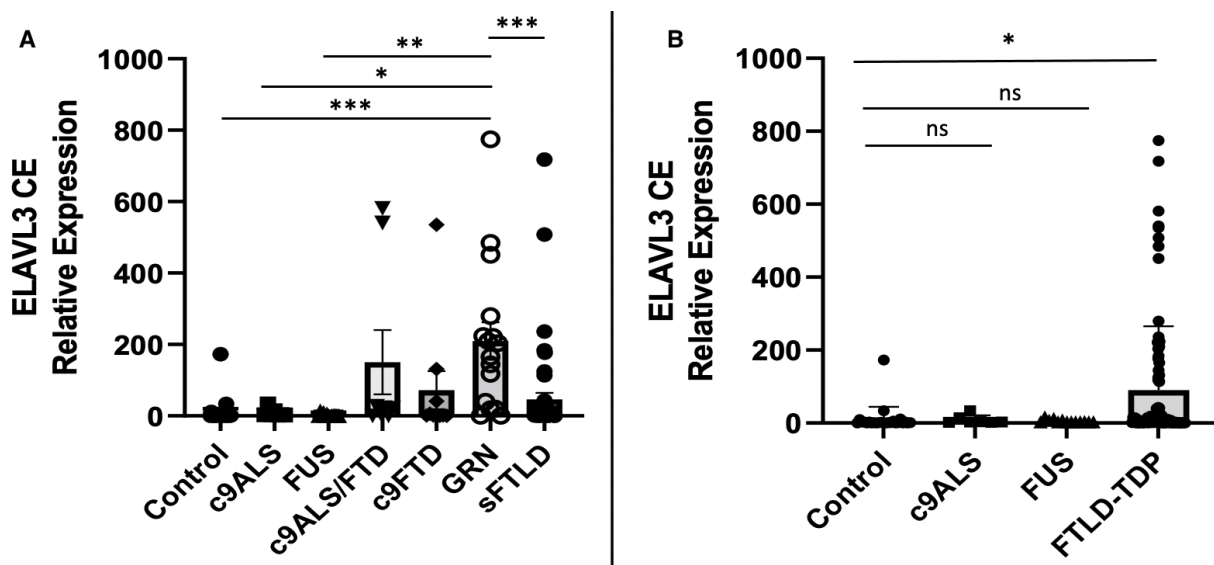


Fig. 4. *ELAVL3* cryptic exon levels correlate with higher TDP-43 pathology.

A) Disease cases include C9ALS/FTD, C9FTD, GRN, and sFTLD; all contain higher relative *ELAVL3* cryptic exon levels (one-way ANOVA, *, **, *** $p < 0.05$, $n = 129$).

B) Disease cases have significantly higher *ELAVL3* cryptic exon levels compared to three control cases (control, c9ALS, FUS) (one-way ANOVA, * $p < 0.05$, $n = 129$).

(Data collected in collaboration with Mingee Chung).

Table 1. TDP-43 pathology is present in four out of six ALS/FTD-related diseases examined in determining *ELAVL3* cryptic exon relative expression.

Disease	TDP-43 Pathology
C9ALS	No
FUS	No
C9ALS/FTD	Yes
C9FTD	Yes
GRN	Yes
sFTD	Yes

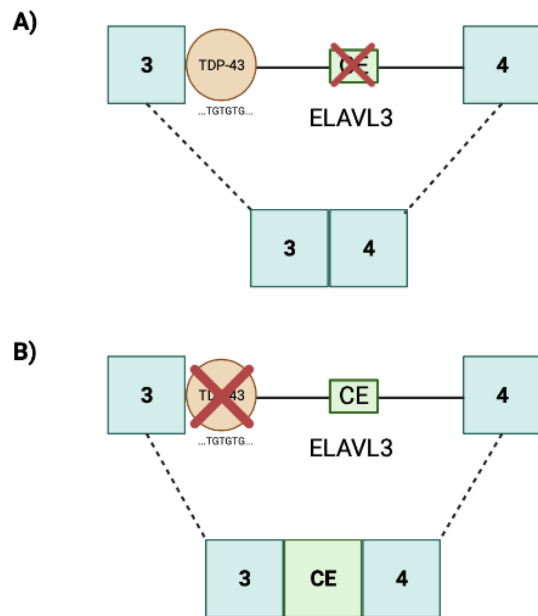


Fig. 5.

A) Wild-type TDP-43 RNA-binding protein allows for alternative splicing of the *ELAVL3* gene; the *ELAVL3* cryptic exon is spliced out of the final mRNA transcript.

B) The loss of TDP-43 (pathological) leads to alternative splicing events, and the *ELAVL3* cryptic exon is included in the final transcript.

References

- Apcher, S., Millot, G., Daskalogianni, C., Scherl, A., Manoury, B., & Fähræus, R. (2013). Translation of pre-spliced RNAs in the nuclear compartment generates peptides for the MHC class I pathway. *Proceedings of the National Academy of Sciences of the United States of America*, *110*(44), 17951–17956. <https://doi.org/10.1073/pnas.1309956110>
- Arai, T., Hasegawa, M., Akiyama, H., Ikeda, K., Nonaka, T., Mori, H., Mann, D., Tsuchiya, K., Yoshida, M., Hashizume, Y., & Oda, T. (2006). TDP-43 is a component of ubiquitin-positive tau-negative inclusions in frontotemporal lobar degeneration and amyotrophic lateral sclerosis. *Biochemical and biophysical research communications*, *351*(3), 602–611. <https://doi.org/10.1016/j.bbrc.2006.10.093>
- Buratti, E., Brindisi, A., Giombi, M., Tisminetzky, S., Ayala, Y. M., & Baralle, F. E. (2005). TDP-43 binds heterogeneous nuclear ribonucleoprotein A/B through its C-terminal tail: an important region for the inhibition of cystic fibrosis transmembrane conductance regulator exon 9 splicing. *The Journal of biological chemistry*, *280*(45), 37572–37584. <https://doi.org/10.1074/jbc.M505557200>
- Cai, H., Zheng, D., Yao, Y., Yang, L., Huang, X., & Wang, L. (2022). Roles of Embryonic Lethal Abnormal Vision-Like RNA Binding Proteins in Cancer and Beyond. *Frontiers in cell and developmental biology*, *10*, 847761. <https://doi.org/10.3389/fcell.2022.847761>
- Cooper-Knock, J., Shaw, P. J., & Kirby, J. (2014). The widening spectrum of C9ORF72-related disease; genotype/phenotype correlations and potential modifiers of clinical phenotype. *Acta neuropathologica*, *127*(3), 333–345. <https://doi.org/10.1007/s00401-014-1251-9>
- DeJesus-Hernandez, M., Mackenzie, I. R., Boeve, B. F., Boxer, A. L., Baker, M., Rutherford, N. J., Nicholson, A. M., Finch, N. A., Flynn, H., Adamson, J., Kouri, N., Wojtas, A., Sengdy, P., Hsiung, G. Y., Karydas, A., Seeley, W. W., Josephs, K. A., Coppola, G., Geschwind, D. H., Wszolek, Z. K., ... Rademakers, R. (2011). Expanded GGGGCC hexanucleotide repeat in noncoding region of C9ORF72 causes chromosome 9p-linked FTD and ALS. *Neuron*, *72*(2), 245–256. <https://doi.org/10.1016/j.neuron.2011.09.011>
- Diaz-Garcia, S., Ko, V. I., Vazquez-Sanchez, S., Chia, R., Arogundade, O. A., Rodriguez, M. J., Traynor, B. J., Cleveland, D., & Ravits, J. (2021). Nuclear depletion of RNA-binding protein ELAVL3 (HuC) in sporadic and familial amyotrophic lateral sclerosis. *Acta neuropathologica*, *142*(6), 985–1001. <https://doi.org/10.1007/s00401-021-02374-4>
- Dugger, B. N., & Dickson, D. W. (2017). Pathology of Neurodegenerative Diseases. *Cold*

- Spring Harbor perspectives in biology*, 9(7), a028035.
<https://doi.org/10.1101/cshperspect.a028035>
- Dvinge, H., & Bradley, R. K. (2015). Widespread intron retention diversifies most cancer transcriptomes. *Genome medicine*, 7(1), 45. <https://doi.org/10.1186/s13073-015-0168-9>
- Ferrari, R., Kapogiannis, D., Huey, E. D., & Momeni, P. (2011). FTD and ALS: a tale of two diseases. *Current Alzheimer research*, 8(3), 273–294.
<https://doi.org/10.2174/156720511795563700>
- Ghasemi, M., & Brown, R. H., Jr (2018). Genetics of Amyotrophic Lateral Sclerosis. *Cold Spring Harbor perspectives in medicine*, 8(5), a024125.
<https://doi.org/10.1101/cshperspect.a024125>
- Grassi, E., Santoro, R., Umbach, A., Grosso, A., Oliviero, S., Neri, F., Conti, L., Ala, U., Provero, P., DiCunto, F., & Merlo, G. R. (2019). Choice of Alternative Polyadenylation Sites, Mediated by the RNA-Binding Protein Elavl3, Plays a Role in Differentiation of Inhibitory Neuronal Progenitors. *Frontiers in cellular neuroscience*, 12, 518.
<https://doi.org/10.3389/fncel.2018.00518>
- Hasegawa, M., Arai, T., Nonaka, T., Kametani, F., Yoshida, M., Hashizume, Y., Beach, T. G., Buratti, E., Baralle, F., Morita, M., Nakano, I., Oda, T., Tsuchiya, K., & Akiyama, H. (2008). Phosphorylated TDP-43 in frontotemporal lobar degeneration and amyotrophic lateral sclerosis. *Annals of neurology*, 64(1), 60–70. <https://doi.org/10.1002/ana.21425>
- Iborra, F. J., Jackson, D. A., & Cook, P. R. (2001). Coupled transcription and translation within nuclei of mammalian cells. *Science (New York, N.Y.)*, 293(5532), 1139–1142.
<https://doi.org/10.1126/science.1061216>
- Kabashi, E., Lin, L., Tradewell, M. L., Dion, P. A., Bercier, V., Bourgouin, P., Rochefort, D., Bel Hadj, S., Durham, H. D., Vande Velde, C., Rouleau, G. A., & Drapeau, P. (2010). Gain and loss of function of ALS-related mutations of TARDBP (TDP-43) cause motor deficits in vivo. *Human molecular genetics*, 19(4), 671–683.
<https://doi.org/10.1093/hmg/ddp534>
- Lee, S., Wei, L., Zhang, B., Goering, R., Majumdar, S., Wen, J., Taliaferro, J. M., & Lai, E. C. (2021). ELAV/Hu RNA binding proteins determine multiple programs of neural alternative splicing. *PLoS genetics*, 17(4), e1009439.
<https://doi.org/10.1371/journal.pgen.1009439>
- Ling, J. P., Pletnikova, O., Troncoso, J. C., & Wong, P. C. (2015). TDP-43 repression of

- nonconserved cryptic exons is compromised in ALS-FTD. *Science (New York, N.Y.)*, 349(6248), 650–655. <https://doi.org/10.1126/science.aab0983>
- Ling, S. C., Polymenidou, M., & Cleveland, D. W. (2013). Converging mechanisms in ALS and FTD: disrupted RNA and protein homeostasis. *Neuron*, 79(3), 416–438. <https://doi.org/10.1016/j.neuron.2013.07.033>
- Lomen-Hoerth, C., Murphy, J., Langmore, S., Kramer, J. H., Olney, R. K., & Miller, B. (2003). Are amyotrophic lateral sclerosis patients cognitively normal?. *Neurology*, 60(7), 1094–1097. <https://doi.org/10.1212/01.wnl.0000055861.95202.8d>
- Ma, X. R., Prudencio, M., Koike, Y., Vatsavayai, S. C., Kim, G., Harbinski, F., Briner, A., Rodriguez, C. M., Guo, C., Akiyama, T., Schmidt, H. B., Cummings, B. B., Wyatt, D. W., Kurylo, K., Miller, G., Mekhoubad, S., Sallee, N., Mekonnen, G., Ganser, L., Rubien, J. D., ... Gitler, A. D. (2022). TDP-43 represses cryptic exon inclusion in the FTD-ALS gene UNC13A. *Nature*, 603(7899), 124–130. <https://doi.org/10.1038/s41586-022-04424-7>
- Mackenzie, I. R., & Rademakers, R. (2008). The role of transactive response DNA-binding protein-43 in amyotrophic lateral sclerosis and frontotemporal dementia. *Current opinion in neurology*, 21(6), 693–700. <https://doi.org/10.1097/WCO.0b013e3283168d1d>
- Masrori, P., & Van Damme, P. (2020). Amyotrophic lateral sclerosis: a clinical review. *European journal of neurology*, 27(10), 1918–1929. <https://doi.org/10.1111/ene.14393>
- Mendez, M. F., Joshi, A., Tassniyom, K., Teng, E., & Shapira, J. S. (2013). Clinicopathologic differences among patients with behavioral variant frontotemporal dementia. *Neurology*, 80(6), 561–568. <https://doi.org/10.1212/WNL.0b013e3182815547>
- Neumann, M., Sampathu, D. M., Kwong, L. K., Truax, A. C., Micsenyi, M. C., Chou, T. T., Bruce, J., Schuck, T., Grossman, M., Clark, C. M., McCluskey, L. F., Miller, B. L., Masliah, E., Mackenzie, I. R., Feldman, H., Feiden, W., Kretzschmar, H. A., Trojanowski, J. Q., & Lee, V. M. (2006). Ubiquitinated TDP-43 in frontotemporal lobar degeneration and amyotrophic lateral sclerosis. *Science (New York, N.Y.)*, 314(5796), 130–133. <https://doi.org/10.1126/science.1134108>
- Ogawa, Y., Kakumoto, K., Yoshida, T. *et al.* Elavl3 is essential for the maintenance of Purkinje neuron axons. *Sci Rep* 8, 2722 (2018). <https://doi.org/10.1038/s41598-018-21130-5>
- Onyike, C. U., & Diehl-Schmid, J. (2013). The epidemiology of frontotemporal dementia.

International review of psychiatry (Abingdon, England), 25(2), 130–137.
<https://doi.org/10.3109/09540261.2013.776523>

Phukan, J., Pender, N. P., & Hardiman, O. (2007). Cognitive impairment in amyotrophic lateral sclerosis. *The Lancet. Neurology*, 6(11), 994–1003. [https://doi.org/10.1016/S1474-4422\(07\)70265-X](https://doi.org/10.1016/S1474-4422(07)70265-X)

Polymenidou, M., Lagier-Tourenne, C., Hutt, K. R., Huelga, S. C., Moran, J., Liang, T. Y., Ling,

S. C., Sun, E., Wancewicz, E., Mazur, C., Kordasiewicz, H., Sedaghat, Y., Donohue, J. P., Shiue, L., Bennett, C. F., Yeo, G. W., & Cleveland, D. W. (2011). Long pre-mRNA depletion and RNA missplicing contribute to neuronal vulnerability from loss of TDP-43. *Nature neuroscience*, 14(4), 459–468. <https://doi.org/10.1038/nn.2779>

Prasad, A., Bharathi, V., Sivalingam, V., Girdhar, A., & Patel, B. K. (2019). Molecular

Mechanisms of TDP-43 Misfolding and Pathology in Amyotrophic Lateral Sclerosis. *Frontiers in molecular neuroscience*, 12, 25. <https://doi.org/10.3389/fnmol.2019.00025>

Schwenk, B. M., Hartmann, H., Serdaroglu, A., Schludi, M. H., Hornburg, D., Meissner, F.,

Orozco, D., Colombo, A., Tahirovic, S., Michaelson, M., Schreiber, F., Haupt, S., Peitz, M., Brüstle, O., Küpper, C., Klopstock, T., Otto, M., Ludolph, A. C., Arzberger, T., Kuhn, P. H., ... Edbauer, D. (2016). TDP-43 loss of function inhibits endosomal trafficking and alters trophic signaling in neurons. *The EMBO journal*, 35(21), 2350–2370. <https://doi.org/10.15252/embj.201694221>

Shodai, A., Morimura, T., Ido, A., Uchida, T., Ayaki, T., Takahashi, R., Kitazawa, S., Suzuki,

S., Shirouzu, M., Kigawa, T., Muto, Y., Yokoyama, S., Takahashi, R., Kitahara, R., Ito, H., Fujiwara, N., & Urushitani, M. (2013). Aberrant assembly of RNA recognition motif 1 links to pathogenic conversion of TAR DNA-binding protein of 43 kDa (TDP-43). *The Journal of biological chemistry*, 288(21), 14886–14905. <https://doi.org/10.1074/jbc.M113.451849>

Soller, M., & White, K. (2004). ELAV. *Current biology : CB*, 14(2), R53. <https://doi.org/10.1016/j.cub.2003.12.041>

Tollervey, J. R., Curk, T., Rogelj, B., Briese, M., Cereda, M., Kayikci, M., König, J.,

Hortobágyi, T., Nishimura, A. L., Zupunski, V., Patani, R., Chandran, S., Rot, G., Zupan, B., Shaw, C. E., & Ule, J. (2011). Characterizing the RNA targets and position-dependent splicing regulation by TDP-43. *Nature neuroscience*, 14(4), 452–458. <https://doi.org/10.1038/nn.2778>

Wang, H. Y., Wang, I. F., Bose, J., & Shen, C. K. (2004). Structural diversity and functional

implications of the eukaryotic TDP gene family. *Genomics*, 83(1), 130–139.
[https://doi.org/10.1016/s0888-7543\(03\)00214-3](https://doi.org/10.1016/s0888-7543(03)00214-3)